Nanoscale Advances

ROYAL SOCIETY OF CHEMISTRY

PAPER

View Article Online
View Journal | View Issue

Cite this: *Nanoscale Adv.*, 2025, **7**, 1163

A color-coordinated approach to the flow synthesis of silver nanoparticles with custom morphologies†

Carly J. Frank, Connor R. Bourgonje, Mahzad Yaghmaei and Juan C. Scaiano *

In an effort to meet the high demand for silver nanostructures in both research and consumer applications, we devise a simple and readily scaleable photochemical method through which silver nanostructures of varying morphologies, sizes, and optical properties can be synthesized using batch and flow photochemical strategies. For the latter we build upon the application of a wrapped-lamp photochemical flow system recently developed by our group to enable sequential irradiation with several wavelengths of LEDs in series in an approach that we describe as "plasmon pushing". We find that this strategy can accelerate the conversion of silver nanoparticle seeds to decahedral and triangular nanostructures, and that with it we have control over the tuning of the size and optical properties of triangular nanostructures in the red and near-IR regions. Moreover, through sequential flow irradiation, we gain a better understanding of the formation pathways and relative stability of decahedral and triangular silver nanostructures.

Received 15th November 2024
Accepted 18th December 2024

DOI: 10.1039/d4na00941j

rsc.li/nanoscale-advances

Introduction

With strong surface plasmon resonance characteristics, silver nanoparticles (AgNPs) and nanostructures have found applications in catalysis and spectroscopy and as antibacterial agents in various industries and consumer goods.[1–3] Synthesizing and applying such structures is an active field of study.[4–6] As a result, various chemical synthesis methods have been found to generate silver nanoparticles, albeit typically on a small scale.[7] With increasing applications, developing simple and easily scalable production methods for these nanostructures is essential. Recently, our group developed a simple photochemical flow setup to generate a continuous stream of AgNP "seeds", facilitating scale-up.[8] These AgNP seeds are small (<10 nm) and roughly spherical, with absorbance typically around 400 nm.[8] Most importantly, they are highly photosensitive, such that even a few hours of light exposure can cause them to shift into new, amorphic structures.[9] Earlier research by our group has found that irradiating seeds with light-emitting diodes (LEDs) at specific wavelengths in the visible region can alter their morphology and size, giving rise to interesting shapes[10] including decahedra and very thin triangular plates.[9] Such changes also alter the absorption characteristics of the nanostructures, making them ideal for specialized applications, such as photocatalysts and colorimetric sensors.[11–13] However, the synthesis of these complex morphologies is very time consuming using the current photochemical methods, and light-free approaches often rely on bulky surfactants or polymers.[14,15]

The characteristic surface plasmon resonance bands of spherical noble metal nanoparticles such as silver and gold are usually at ~400 nm and ~530 nm, respectively. However, these plasmon bands change dramatically when the morphology, size or aspect ratio is changed.[16–18] This has significant implications for the absorbance and optical properties of AgNPs and therefore their applications.[9,19,20] One of the most popular and longstanding uses of silver, for instance, has been as an antibacterial agent.[1–3,21–23] Related to this, research has also been done on the exploitation of easily excitable surface plasmon resonance bands to enhance AgNP bactericidal activity through irradiation with specific wavelengths of light.[2,15] From studies on this morphological dependence on the antibacterial capabilities of AgNPs, it has been found that triangular AgNPs (tAgNPs) are among the most potent antibacterial agents among common AgNPs when activated with light.[2,21] Furthermore, tAgNPs are very promising for biological applications, such as photodynamic therapy, because their absorbances can often be tuned to lie within the biological window of 650 to 1350 nm.[24] This is a consequence of the sharp edges and vertices whereat electrons can respond to low-frequency electric fields in the late visible and IR regions.[25] Similarly, decahedral AgNPs (dAgNPs) were found to perform very well when irradiated with blue light, as this overlaps with their characteristic absorption at approximately 480–520 nm.[2]

Department of Chemistry and Biomolecular Sciences, University of Ottawa, Ottawa, Ontario, K1N 6N5, Canada. E-mail: jscaiano@uottawa.ca

† Electronic supplementary information (ESI) available: Details and photographs of the experimental set-up, additional spectral and TEM data and details of particle size distribution. See DOI: https://doi.org/10.1039/d4na00941j

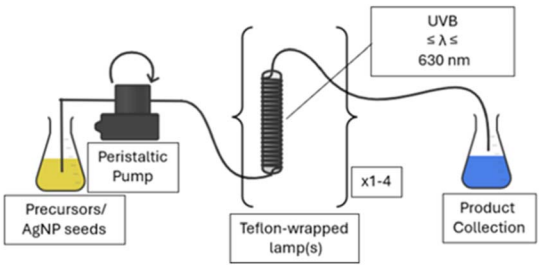

Fig. 1 Generalized diagram of the photochemical flow setup utilized in this study. The identity of each lamp varied depending on the desired outcome, with UVB being used to generate AgNP seeds from a precursor solution and visible LEDs of varying wavelengths to transform seeds into d and tAgNPs. A photograph of the true system is available in the ESI (Fig. S6).†

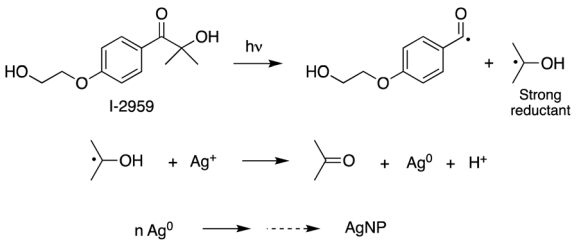

Scheme 1 Norrish type I cleavage of I-2959 following UV photoexcitation and a subsequent PCET reaction between the ketyl radical and a silver cation to form one equivalent of reduced silver that spontaneously aggregates to form AgNPs.

In this contribution we develop a photochemical synthesis strategy using a sequence of multiple visible light wavelengths (see Fig. S1†) in flow to generate decahedral and triangular silver nanostructures, significantly reducing the time required to achieve the desired morphology from seeds and to produce them consistently with reliable morphologies. Adapted from an earlier study by our group,[26] this simple photochemical flow setup consists of a peristaltic pump used to pump solution through thin Teflon tubing wrapped around one or several lamps of different wavelengths, depending on the desired outcome. Fig. 1, below, provides a diagram of the typical setup. The setup occupies little space, utilizing lamps which are 1 foot in length in an expo panel which can accommodate up to 5 lamps at once.

As will be discussed, our system moves from the typical monochromatic irradiation to generate modified structures with absorbances at the LED emission wavelength to a sequential irradiation system, better facilitating absorption of light by the starting structures. This enables "plasmon pushing", in which plasmon absorbance is gradually shifted towards longer wavelengths through either irradiation with progressively longer wavelengths of light or longer irradiation time, essentially tracking the absorbance of AgNPs as they progress to different morphologies with absorbances at longer wavelengths. Sequential irradiation enables an overall faster transformation as there is less of a gap between the absorbance of the starting AgNPs and the emission of the light source, thus better satisfying the first law of photochemistry which requires light absorption by the reactants as a precondition for any photochemical change to take place.[27] Moreover, the faster product formation in combination with the nature of the flow setup enables a continuous stream of nanoparticles to be generated in a matter of hours. Our studies lead to an improved understanding of the pathways taken in forming decahedral and triangular silver nanostructures.

Results

The synthesis of AgNPs is typically done using a bottom-up approach,[28] beginning from a source of Ag^+ ions such as silver nitrate ($AgNO_3$).[8,9,18,29] The initial structures that form are often AgNP "seeds" – small, roughly spherical nanostructures ranging from one to tens of nanometers in diameter. These seeds have characteristic absorbance at approximately 400 nm, and their solutions are easily identified by their light yellow colour. In a recent publication, we showed that AgNP seed synthesis is amenable to flow photochemical strategies with a range of different photoinitiators.[8]

Here, we take advantage of the observation that AgNP seeds serve as building blocks for more complex morphologies,[2,9] which typically increase in size and/or aspect ratio as their absorbances shift into longer-wavelength regions of the vis-NIR spectrum. LEDs offer some key advantages over traditional fluorescent lamps, being widely accessible, cost and energy efficient, and safer and having highly selective emissions.[9] Our strategy is chemically quite simple, utilizing an Irgacure-2959 (I-2959) as a highly efficient photoinitiator and citrate as a stabilizer that can also assist the Ag^+ reduction process.[8] The citrate concentration was selected as 1 mM based on earlier studies[2] that showed this to be a convenient, yet low concentration (see also Fig. S2†). The photochemistry of I-2959 and the initial reduction of Ag^+ are illustrated in Scheme 1.[30,31]

Preliminary batch experiments and scale up

Experiments to manufacture dAgNPs and tAgNPs were performed using 450 nm and 630 nm LED sources, respectively. The photochemical synthesis of d or tAgNPs has been achieved in batches up to 200 mL (see Fig. S4†) by our group. With the simple method utilized by our group,[8,9] it is believed that the main barrier in the reaction efficiency is the inability of the starting seeds to absorb light from the long-wavelength LED sources. This causes the early stages of the morphological conversion to be very slow until they reach a point with enhanced visible absorbance and start to transform from seeds into the desired morphologies. Recalling that AgNP seeds have a typical absorbance of around 400 nm, one can quickly see that a blue LED, with a typical emission of around 450 nm, may overlap weakly with this band (see Fig. S8†); however, a red LED, whose typical emission occurs around 630 nm, has very poor, if any, overlap with this absorption band. Hence, the probability of AgNP seeds absorbing a photon emitted by the red LED is quite low, and thus long irradiation times are often required in order to start and complete the transformation into tAgNPs.

In this work, we also manipulated the citrate concentrations, allowing for further accurate control of the plasmonic absorption properties and AgNP size (Fig. S2 and S3†). Fig. S2† shows that plasmon bands can be tuned within the visible (~650 nm) and NIR (~1300 nm) regions as the concentration of citrate is increased up to 15 mM. Fig. S4† illustrates the change in the plasmon bands as the batch reaction progresses.

Flow-and-rest improved synthesis of AgNP seeds

Initially, a large stock solution of AgNP seeds was prepared using a procedure similar to the one previously published.[8] A UVB lamp double-wrapped with Teflon tubing was used to ensure adequate irradiation and spectral overlap with the I-2959 initiator. The starting solution was pumped through at a speed corresponding to a flow rate of 3.12 mL min^{-1}, for a system residence time of about 7.4 minutes. Using this method, 500 mL of solution was collected in approximately 2.5 h.

Yaghmaei and colleagues[8] found that growth occurs essentially immediately in an inert atmosphere. While experiments confirm this, we have also found that if these conditions are not fully met, growth may be initially impeded. Interestingly, however, slow growth of the seeds does not seem to hinder their further reactivity, nor does it limit their eventual final absorption.

Fig. 2 illustrates the spectra of the product taken throughout the synthesis using a flow cuvette. This solution was bubbled with argon; however, it was not fully devoid of air. While the residence time did not change dramatically throughout the experiment, the characteristic peak of the seeds started small and grew steadily for at least the first hour of the experiment.

The UV-vis absorption spectra show that I-2959, the photoinitiator, had been totally consumed within the residence time;

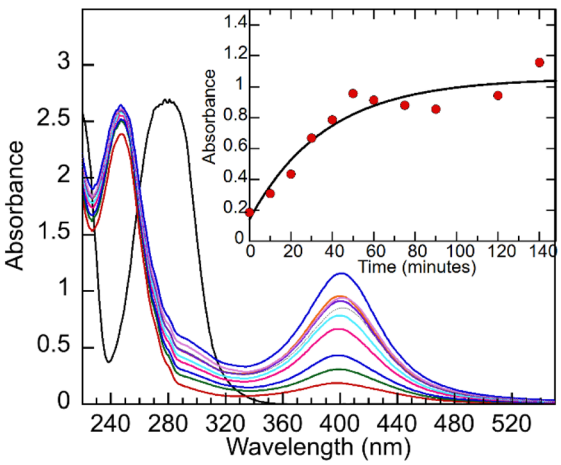

Fig. 2 UV-vis absorbance spectra of synthesized AgNP seeds in single-pass flow under UVB irradiation. The starting solution is shown in black and represents I-2959. The solution collected in-line upon this first appearance is displayed in dark red. Samples were then taken at 10-minute intervals following the first appearance up to one hour and then in 15–20-minute intervals until 140 min. (Inset): Maximum absorbance of sample output *vs.* time after the first appearance of the product during flow synthesis progress. Note that all samples had about 7.4 min residence time in the flow system. The spectral differences simply reflect how long the flow system has been in use.

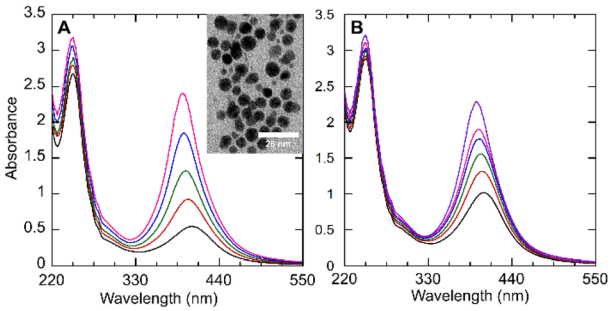

Fig. 3 (A) UV-vis absorbance spectra of bottle 1 seeds, 1 (black), 6 (red), 12 (green), 20 (blue), and 32 (pink) days after synthesis. (B) UV-vis absorbance spectra of bottle 2 seeds 1 (black), 6 (red), 12 (green), 20 (blue), 25 (pink), and 55 (purple) days after synthesis. All seeds were stored in the dark at room temperature between use and spectral measurements. (Inset): the representative TEM image of bottle 1 seeds 20 days post-synthesis. Scale bar: 25 nm. Measurements of 200 bottle 1 seeds gave an average particle diameter of 6 ± 2 nm. See Fig. S12A† for particle distribution histograms.

earlier studies suggest that I-2959 is consumed in less than 40 s even with a single-wrapped lamp.[8] The rest of the spectra all had the same exposure and same residence time (7.4 minutes); all were fresh unreacted samples as they entered the flow region, and all absorbances were measured in less than 30 s after leaving the illuminated region. Assuming that the solution becomes increasingly saturated with argon as the experiment progresses, one might assume that this growth is merely a reflection of the time required to fully purge the solution. However, as the data presented next suggest, this process does not stop upon exit from the illuminated flow system and subsequent exposure to air.

Due to the volume of the solution being produced, the solution was collected and stored in two amber bottles – the first held the first half of the synthesis, which had generally lower absorbances when measured in-line, while the second held the second half of the synthesis. These bottles were numbered 1 and 2, respectively, and their spectra were measured several times after the initial synthesis to monitor any changes; these results, along with a representative TEM image of the batch, are shown in Fig. 3.

Smaller batches of seeds were later produced after this initial supply had been exhausted; the spectrum of the final batch over time along with a TEM image of the seeds is provided in Fig. S5.†

The fact that the plasmon peak grows long after I-2959 has been consumed and well after UV exposure is complete, but that both the initiator and light are initially needed, suggests the formation of a catalyst that remains in the system and catalyzes the formation of more nanoparticles. Such an autocatalytic process is reminiscent of processes in B/W photography[32] where silver clusters are part of the latent image, later developed in the dark and assisted by mild reducing agents.

Decahedral silver nanoparticles (dAgNPs) from seeds

To form dAgNPs, seeds were pumped through Teflon tubing doubly wrapped around a blue LED (λ = 455 nm). A goal

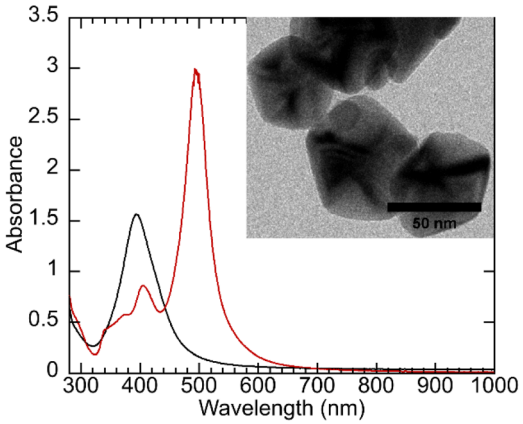

Fig. 4 UV-vis absorbance spectra of a single pass of AgNP seeds through a double-wrapped blue LED (λ = 455 nm). The spectrum of initial seeds is shown in black, and the product is shown in red. Residence time was approximately 3.3 hours. (Inset): TEM image of the product from single pass flow of AgNP seeds through a double-wrapped blue LED. Contrast and sharpness have been adjusted for image clarity. Scale bar: 50 nm. For lamp emission spectra, see Fig. S1.†

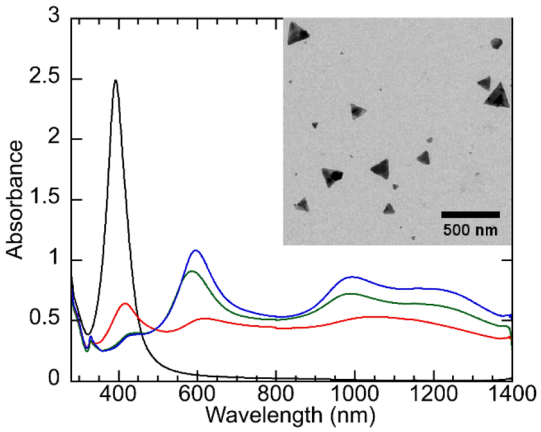

Fig. 5 UV-vis-NIR absorbance spectra for the slow cyclic flow of AgNP seeds (black) through a series of 4 single wrapped green LEDs (λ = 522 nm), with approximate exposure times of 31.3 h (red), 63 h (green), and 72 h (blue). (Inset): the TEM image of the final product from cyclic flow of AgNP seeds through green LEDs, following 72 h of exposure. Contrast and brightness have been adjusted for image clarity. Scale bar: 500 nm. For lamp emission spectra, see Fig. S1.†

residence time of 3–4 hours was set based on the results from a cyclic reaction which will be discussed later (Fig. 9). The results of the single pass experiment with a residence time of approximately 3.3 h are displayed in Fig. 4, and a selected TEM image of the product is shown in the inset.

Formation of triangular silver nanoplates (tAgNPs) from seeds using a green LED

As an alternative to long-wavelength red LED irradiation, and following the idea of plasmon pushing, AgNP seeds were pumped slowly through the same series of 4 single wrapped green LEDs as used above. The solution was recycled several times to prolong the total exposure with very little dead volume in this setup. The results of this experiment are displayed in Fig. 5 and the inset displays a TEM image of the final collected product after a total of 72 h of exposure. Note that there is no defined peak in the 500 nm region characteristic of decahedra.

Formation of triangular silver nanoplates (tAgNPs) from seeds using warm white, amber, and red LEDs

To act as an intermediate between the short-wavelength absorbance of the starting seeds and the long-wavelength emission of red LED, seeds were pumped once through a double-wrapped warm white LED (wwLED), with gentle cooling to maintain the temperature of the tube below 35 °C, in the hope that this would accelerate the initial process leading to tAgNPs. Again, we thought that the ~450 nm band of the wwLED (see Fig. S1† for lamp emission spectra) would help initiate the plasmon pushing process. The residence time of this single pass was 5 h. Following that, the resulting solution was divided into two parts: the first half continued to be recycled through the wwLED, while the second half was recycled through a double-wrapped red LED. The results of this experiment are displayed in Fig. 6. The recycling portion was done so as to correspond to an exposure time of an additional 18 h. The total exposure times were 23 h under warm white, or 5 h under warm white followed by 18 h under red. Several insets (or panels) display selected TEM images from (i) a single pass through warm white, (ii) 23 h of exposure to warm white, and (iii) 5 h of exposure to warm white plus 18 h of exposure to red.

To move from recycling to a preferred uninterrupted single pass, double wrapped warm white, amber, and red LEDs were

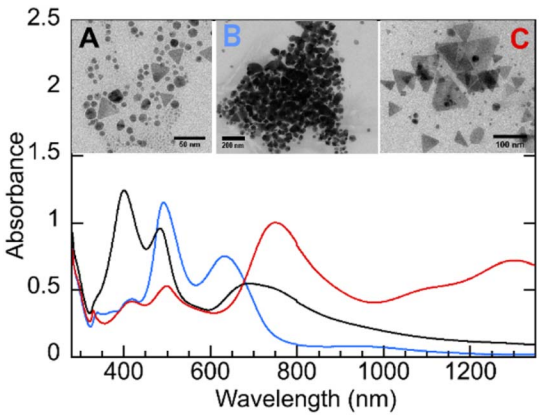

Fig. 6 UV-vis-NIR absorbance spectra of AgNP seeds after a single pass flow through a double-wrapped warm white LED (451 nm, 602 nm br.) (black). After this single pass, some solution was cycled through the warm white for an additional 18 h of exposure (blue), while the rest was cycled through a double-wrapped red LED (λ = 632 nm) for 18 h of exposure (red). Insets (A) TEM image of AgNP seeds after a single pass (~5 h) through the warm white LED. Contrast and brightness have been adjusted for image clarity. Scale bar: 50 nm; (B) TEM image of AgNP seeds after a total of ~23 h of exposure to the warm white LED in flow. Scale bar: 200 nm; (C) TEM image of AgNP seeds after approximately 5 h of exposure to warm the white LED followed by 18 h of exposure to a red LED in flow. Contrast and brightness have been adjusted for image clarity. Scale bar: 100 nm.

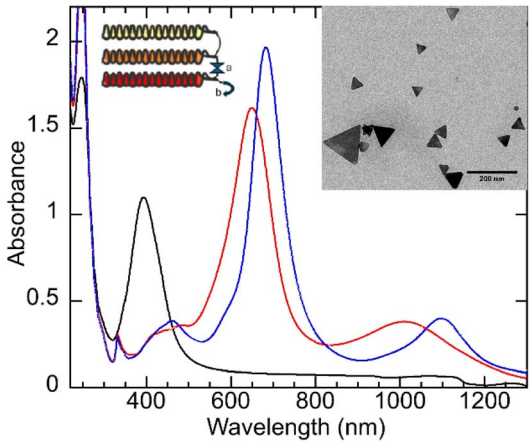

Fig. 7 UV-vis-NIR absorbance spectra of AgNP seeds (black) pumped in a single pass sequentially through warm white (451 nm, 602 nm br.), amber ($\lambda = 590$ nm), and red ($\lambda = 632$ nm) LEDs. The warm white + amber in-line sample is shown in red; the collected product from warm white, amber, and red is shown in blue. For visualization purposes, a scheme of the setup is shown in the inset (left), where "a" corresponds to the sample location of the red plot (9.1 h of residence time) and b corresponds to the sample location of the blue plot (14.1 h of residence time). (Right inset): The TEM image of the product after AgNP seeds were flown in a single pass through a series of double wrapped warm white, amber, and red LEDs (blue curve). Contrast and brightness have been adjusted for image clarity. Scale bar: 200 nm.

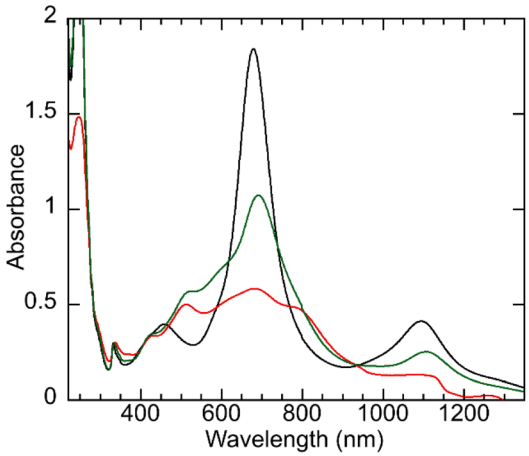

Fig. 8 UV-vis-NIR results of pumping a solution of tAgNPs (black) through a double-wrapped bLED, with a residence time of ~5.6 hours. Two temperature conditions were tested, modified by cooling the outside of the tube with a light stream of air during synthesis to maintain the system at approximately room temperature (green), and without temperature control, in which the outer temperature of the lamp reached 55 °C (red). For lamp emission spectra, see Fig. S1.†

connected in series. Seed solution was pumped through them starting from the warm white, then amber, and then red, in order of increasing wavelength of peak emission under the basis of plasmon pushing previously discussed. The product was collected and sampled, and at one point a sample was taken from between the amber lamp and the red lamp for comparison. The residence time of the solution through all three lamps was approximately 14.1 h, while the residence time of the solution through the warm white and amber lamps only was approximately 9.1 h. The results are displayed in Fig. 7, and are accompanied by a selected TEM image of the final product from all three lamps; in all cases, the flow is about 5 mL h^{-1}.

Photochemical stability of new AgNP morphologies

As the decahedra were found to form reasonably quickly using the single-pass flow system, their photostability was tested by pumping a solution of decahedra through a series of four single-wrapped green LEDs ($\lambda = 522$ nm). The solution was cycled several times at different flow rates in an attempt to maximize the total exposure time. The results of this experiment are displayed in the ESI (Fig. S9).† While some spectral shifts are observed, overall, it is evident that the Ag decahedra are rather robust structures, less prone to photoinitiated modification than the other structures presented here.

Intrigued by the plasmon pushing apparent in tAgNP synthesis, we repeated the warm white-amber-red series experiment in Fig. 7 with a double wrapped blue LED inserted before the warm white lamp, as we now knew that this would first transform all or most of the AgNPs into decahedra, which may then decrease the polydispersity that is suggested by the single pass warm white spectrum (Fig. 6). However, the resulting solution was orange in colour, resembling that of dAgNP solutions previously achieved using only a blue LED. This suggested qualitatively that the warm white, amber, and red LED lamps had little effect on a solution of dAgNPs which we presume formed early in this flow experiment. This spectrum is provided in Fig. S7.† This experiment along with the stability of dAgNPs to prolonged green LED exposure suggests that decahedra are thermodynamically stable, robust structures.

To investigate the relative stability of tAgNPs compared to dAgNPs, we irradiated a solution of tAgNPs, synthesized using the wwLED + amber LED + red LED series (Fig. 7), with a blue LED with and without gentle cooling in air. The results of this are provided in Fig. 8 and suggest that tAgNPs do not have the stability that was observed for dAgNPs. In contrast, they degrade at a temperature-dependent rate. The data at 55 °C show a peak growing at ~500 nm, suggesting the initial formation of dAgNPs or unstable structures that may eventually lead to thermodynamically preferred morphologies.

Formation studies of complex AgNP morphologies

Cyclic flow reactions were conducted to approximate the required exposure time required to yield an acceptable transformation into dAgNPs and tAgNPs. In flow recycles, the pump is set higher to result in a shorter residence time per pass and the outlet is directed back to the reagent flask. While this results in dead volume in each cycle, which is accounted for when calculating residence time, it provides a good starting point for the transition to single-pass and also allows for UV-vis absorption monitoring and sampling of intermediate solutions to track the growth patterns of the nanostructures.

To convert seeds to decahedra, a blue LED lamp ($\lambda = 455$ nm, see the ESI†) was double wrapped with Teflon tubing. The results are displayed below in Fig. 9, with a TEM image of the

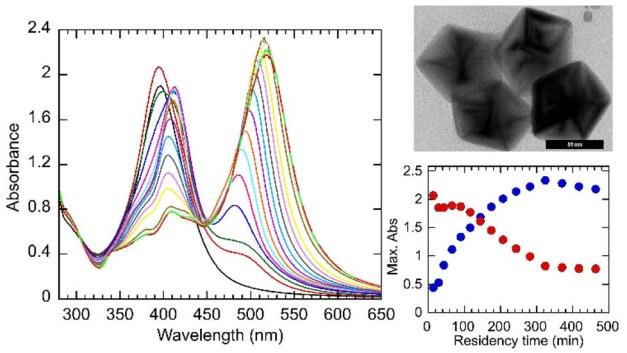

Fig. 9 UV-vis absorbance spectra recorded throughout the cyclic flow of AgNP seeds through a double wrapped blue LED ($\lambda = 455$ nm). Selected lines: starting seed solution (black), 43 minutes of exposure (dark blue), 2 h (purple), 4 h (yellow), 5.4 h (brown), and 7.75 h (final sample) (dashed red). Panels: (upper) the TEM image of the final sample from the cyclic flow of seeds after 7.75 h of exposure. (Scale bar: 50 nm); (lower) Plot of maximum absorbances of shrinking (~400 nm) (red) and growing (~500 nm) (blue) peaks with residence time in the flow system. For lamp emission spectra, see Fig. S1.† See Fig. S12B† for particle distribution histograms.

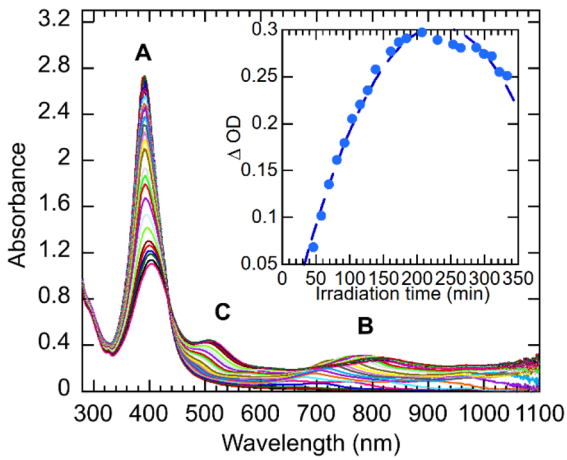

Fig. 10 UV-vis-NIR absorbance spectra of cyclic irradiation of seeds through a double wrapped warm white LED. Spectra were measured every 15–30 minutes in a flow cuvette. Of the 30 mL in the cycle, 23 mL was irradiated at any given point in time, while the remaining 7 mL comprised the dead volume. The regions are labelled A, B, and C in order of spectral appearance.

collected product in the inset. While the irradiation was performed for 7.75 h, the synthesis is essentially completed in 4 h. For photographs showing the appearance of these and other particle solutions, see Fig. S11.†

To achieve more insight on tAgNP formation, a similar cyclic experiment to that described above for dAgNPs was performed using the double-wrapped warm white lamp. The results of this experiment are displayed below in Fig. 10.

Discussion

TEM images of bottle 1 were obtained 20 days after initial synthesis when spectral measurements indicated seed growth was nearing completion; the seeds were measured to be on average 6 ± 2 nm in diameter. Nevertheless—and quite fortunately—the synthesis of dAgNPs or tAgNPs can proceed efficiently one day after seed preparation, even if ripening is not complete.

The first law of photochemistry requires light absorption by the reactants as a precondition for any photochemical change to take place.[27] This condition is fulfilled when the synthesis of decahedra is performed using a blue LED lamp, where seeds absorb about 8.3% of the LED light (see Fig. S8†). This overlap improves as intermediate structures absorbing at longer wavelengths are formed. For example, in the flow recycling experiment with a blue LED to form dAgNPs (see Fig. 9), a new peak forms at 481 nm and gradually (7.7 h) shifts to 518 nm for dAgNPs measuring on average 69 ± 7 nm from the base to the opposite tip. Their spectrum also shows a weak band at ~409 nm, likely due to a transversal plasmonic absorption; we find that absorbance in this region is common to many morphologies.[9]

While recycling tests provide a useful tool to monitor the progress of the reaction, single pass flow photochemistry is more amenable to scale-up. A single pass of AgNP seeds through blue LED irradiation with a 3–4 h residence time without air cooling reached a temperature of 60 °C and produced rather monodisperse decahedral structures measuring 56 ± 7 nm from the base to the opposing tip, slightly smaller in size than those formed more slowly in the cooling cyclic experiment. After a short ripening period (*e.g.*, one day), these structures are very stable and even prolonged irradiation with a 522 nm green LED has little effect (Fig. S9†). This suggests that dAgNPs are largely photostable.

In the synthesis of tAgNPs, a broad spectrum visible lamp such as the warm white LED used here seems key to promoting faster conversion. We note that keeping the warm white lamp below 35 °C produced both dAgNPs and tAgNPs (Fig. 6) after two cycles, while a single uncooled pass through the wwLED favours tAgNP formation. However, with prolonged irradiation with the wwLED, the tAgNP peak broadens and decreases (Fig. 6 and 10), and the dominant structures observed in TEM images consist of dAgNPs or seed-like AgNPs.

In the cyclic warm white experiment (Fig. 10), regions of interest were labelled in their order of appearance as A, the starting seed peak at 400 nm which decayed linearly with time; B, a growing peak in the tAgNP region of ~600–700 nm which appeared very early but whose growth levelled off and slowed in a near-parabolic fashion (Fig. 10 inset); and C, a steadily growing peak in the dAgNP region. To better visualize the growth of these new peaks, the absorbance of the starting seeds was subtracted from the subsequent absorbance spectra measured throughout the recycling, generating a graph of the change in optical density (ΔOD) with respect to the wavelength (see ESI, Fig. S13†). From this information, the changes in optical density for the key peak regions as shown in Fig. 10 were plotted with respect to the cyclic irradiation time. These observations support the suggestions of the destruction studies that dAgNPs are more resilient than tAgNPs and that, moreover,

one is not necessarily an intermediate structure in the formation pathway to the other, as both can grow simultaneously.

Previous studies have reported that temperature can be used to promote the twinning of noble metal nanoparticle seeds;[33] thus, the thermal contributions from an uncooled lamp are sufficient in aiding not only in the rate of overall conversion, but also in selecting for tAgNPs.

Ignoring thermal effects and focusing only on photochemical processes, we propose, based on the findings presented in this paper, a formation scheme which at first glance may seem counterintuitive: although nearly full conversion to dAgNPs can be achieved in only a few hours using the wrapped blue lamp flow system presented in Fig. 4, the range of the emission wavelength is rather limited. Meanwhile, at first glance, tAgNPs appear to be more elusive due to the long irradiation times observed in monochromatic systems, such as the green LED flow system – which required 72 hours of flow recycling and produced polydisperse tAgNPs measuring 110 ± 41 nm on average (Fig. 5) – or the direct irradiation of seeds using a red LED which requires 48 hours in batch (Fig. S4†). However, this is merely a direct consequence of the first law of photochemistry: there is a discrepancy between the seed absorbance around 400 nm and the emission of the light source later in the visible region which significantly prolongs the time required to initiate conversion. We note, however, that in the cases of direct irradiation in a flow system using either a green LED (Fig. 5) or red LED (Fig. S14†), no absorbance peak in the dAgNP region appears – the conversion is immediately to tAgNPs.

The stability studies have shown that tAgNPs may be easily degraded by irradiation with a higher energy wavelength (Fig. 8) while dAgNPs are quite resistant to further modification either through plasmon pushing with longer wavelengths or destruction by shorter wavelengths (Fig. S15†). Thus, the formation pathway to tAgNPs may be viewed, simply put, as a bridge: given a wavelength which can mediate the gap between the absorbances of the seeds and the tAgNPs, such as a broad-spectrum warm white LED, tAgNPs will form readily and reasonably quick, although their structures will be relatively unstable, with a transversal band at ~409 nm which can absorb blue light to facilitate destruction. However, warm white LEDs contain a distinct peak in the blue region at ~451 nm, within the small wavelength window required for dAgNP formation. Our findings suggest that dAgNPs are robust nanostructures and reside in a local energy minimum, making it difficult to facilitate their further transformation.

The addition of red and/or amber light to an initial wwLED in series (see Fig. 8) leads to good tAgNPs with low polydispersity and absorbance bands in the red and NIR regions. Whether the sequence is allowed to progress through all lamps or is halted after the wwLED or amber lamp only affects the position of the red and NIR absorption peaks – TEM measurements of tAgNPs collected both after the amber and the red lamp report nearly identical measurements of 47 ± 22 nm and 47 ± 19 nm, respectively. However, this tunability may prove to be very valuable in biological and health-related applications, as these are the regions with significant tissue transparency, and wavelength tunability into the biological window correlates directly with the depth of penetration.

Conclusion

Our results show that flow photochemistry is a viable solution for the scale-up production of silver nanostructures with custom morphologies and optical properties. A similar approach may be useful for nanostructures of other materials. Combining different wavelengths in carefully selected sequences can help with plasmon pushing, leading to choice morphologies and spectral properties, the latter closely related to the dimensions of the nanoparticles, and greatly improved reaction times (19 h in flow *vs.* 48 h in batch, for tAgNPs). Interestingly, multicolor studies also helped us understand the relative stability of silver structures and in particular the fact that decahedra, dAgNPs, show excellent stability, including resistance to prolonged irradiation. Further flow recycling enables growth progress monitoring to determine the extent to which particles can be modified, which is valuable for achieving desirable nanomaterials and learning about potential photosynthesis and degradation pathways.

Finally, we also show that in batch-scale synthesis, triangular structures with excellent antibacterial properties can have their absorption bands tuned to the biological window in the NIR region by modifying the wavelength(s) of light used in irradiation, and/or the concentration of citrate in the solution. For batch synthesis of tAgNPs, their plasmonic absorption can be tuned within the visible and NIR regions by adding citrate (Fig. S2†). tAgNP materials can have dimensions exceeding 100 nm, while their thicknesses usually remain in the 6 to 12 nm range, and feature fairly large size distributions despite having reasonably distinct absorption bands. By comparison, batch synthesis of dAgNPs was less responsive to citrate manipulation and to prolonged green light irradiation under flow conditions. These findings support the notion that dAgNPs are highly stable structures, while tAgNPs are far more sensitive to their reaction conditions.

Experimental

Materials

Silver nitrate (ACS reagent, 99.9+%) was purchased from Alfa Aesar. Trisodium citrate dihydrate (99%) was purchased from Fisher Scientific. Irgacure-2959 (I-2959) was a gift from BASF Chemicals. All water used is distilled or ultra-pure, prepared by purification of deionized water using a Thermo Scientific Barnstead GenPure water purification system (a conductivity of 18 MΩ cm^{-1}).

Seed synthesis

Two different strategies were used for seed synthesis. For the batch synthesis in a flat, transparent plastic vessel, an aqueous solution of 0.2 mM $AgNO_3$, 0.2 mM I-2959, and between 1 and 15 mM trisodium citrate is deaerated for 30 minutes in the dark under a steady flow of argon. The transparent solution is then

illuminated in a Luzchem UV photoreactor under 8 UVA bulbs for 15 minutes, yielding a deep yellow suspension of AgNP seeds with prominent absorbance centred at around 400 nm.

For the flow synthesis, the approach we recently reported was used.[8,26] Briefly, a UVB lamp double-wrapped with Teflon tubing (id 1.5 mm) acted as the photoreactor and sample container. Double wrapped lamps used about 14 m of tubing and held 22 ± 2 mL of solution, while single wrapping used 6.3 m of tubing and held 10 ± 1 mL. Seeds were stored in the dark in amber bottles at room temperature.

The light source for all flow experiments was an Expo panel from Luzchem where up to five light sources, either fluorescent or of the LED type, were installed as needed. Whenever UV sources were used, an Expo panel shield from Luzchem was used for protection.

AgNP growth

Two different approaches were used for AgNP growth depending on whether a batch of flow synthesis was employed.

For the batch synthesis, using the same container as that for seed synthesis, the seed suspensions are exposed to air for 30 minutes in the dark to reoxygenate the solution and ensure that the AgNP seeds are fully formed. After this, the seed suspension is laid flat on either a blue (450 nm) or red (635 nm) 24-LED well-plate illuminator (WPI, by Luzchem Research Inc.) and shaken gently on an orbital shaker, ensuring that solution is consistently disturbed for the duration of the synthesis (Fig. S4†). The samples are then irradiated for 24 h for the blue WPI, or 48 h for the red WPI. Once complete, the particle suspensions are washed *via* centrifugation at 6000 rpm for 60 min and resuspended in ultrapure water. This process is performed three times total before storing the particles in the dark in glass containers. The resulting suspensions are stable for months, even if left on the benchtop – however, they were stored in the dark as a precaution. The dAgNP suspensions have a distinctive bright orange color, while that of the tAgNPs ranges from deep blue to purple depending on the citrate concentration used (see Fig. S4†).

For flow synthesis lamps were wrapped with thin-walled Teflon tubing (ID = 1.5 mm), from Component Supply. LED and UVB lamps and the accompanying expo panels were purchased from Luzchem. A Gilson MiniPuls 3 was used to pump solution through the experimental apparatus.

All lamps were wrapped by hand with Teflon tubing, ensuring that the tubing was not being stretched and pinched. The volume of the irradiated section of tubing was measured with water prior to the use of each lamp to confirm that the wrapping was suitable. Each single wrapped lamp held 10 ± 1 mL, and each double wrapped lamp held 22 ± 2 mL.

The starting AgNP seed solution was synthesized based on the flow method established and described by Yaghmaei and colleagues,[8,26] using I-2959 as the photoinitiator in a solution of $AgNO_3$ and trisodium citrate in distilled water. The solution was purged with argon for 20 minutes before starting, and the UVB lamp, which was double wrapped with Teflon tubing, was allowed to warm up for approximately 15 minutes before beginning the reaction. Air was blown alongside the flow tube to reduce heating. Seeds were stored in the dark in amber bottles at room temperature.

The general procedure following irradiation depended on whether the experiment was single pass or cyclic: the outlet end of the Teflon tube was directed either to a collection flask or back into the flask containing the reactant solution.

Wrapped lamps were placed in an Expo panel and set horizontally in a fume hood to allow complete filling of the tubing. In the cases of the cyclic synthesis with the blue LED, the single pass synthesis with the warm white LED, and the initial seed synthesis, air cooling maintained the maximum temperature at about 45 °C, varying slightly between each lamp. In all experiments, aluminum foil was secured over the lamp(s) to reflect the light back into the system.

Samples for time stamps were taken in-line from the outlet tube, while those of overall solutions were taken from the collected product. In the case of very slow flows, such as the green and the warm white – amber – red series, pumping was stopped and the lamps were turned off and solution was fast pumped just long enough to collect a sufficient amount, usually approximately 2 mL or enough to fill a 1 cm pathlength cuvette, of sample from the outlet tube. The pump direction was then reversed for the same amount of time as was required to fill the sample collection vial. The pump speed was then reset and lamps were turned back on and the experiment continued. Samples were stored in the dark at room temperature, and tAgNPs and dAgNPs are stable for several weeks or months following synthesis.

Characterization

During flow experiments, real-time UV-vis spectra were measured using a Cary-60 up to 1000 nm. For the initial seed synthesis, AgNP solution was pumped out of the reaction vessel, through a quartz flow cell, and back into the collection flask vessel using a peristaltic pump. For the synthesis of new morphologies, a batch cuvette was used to collect samples from the outlet of the reaction vessel, and samples were immediately analyzed using the Cary-60. For cases when near-IR absorbance was of interest, such as in tAgNP syntheses, the absorption spectra of collected samples were analyzed up to 1400 nm using a Cary-7000 within a few days of their synthesis.

XRD analysis was performed on washed seeds, dAgNPs, and tAgNPs by dropping the solutions onto glass microscope cover slips and allowing them to dry. Deposition was repeated several times to ensure an adequate amount of nanoparticles. XRD measurements of plain microscope covers were also taken and subtracted as a baseline from the nanoparticle plots. These XRD plots are available in the ESI in Fig. S16.† Measurements were conducted using a Bruker D8 Endeavor and peaks were compared to those reported previously by our group.[2] A sharp 111 peak, suggesting high crystallinity despite small NP size, was present in seed, dAgNP, and tAgNP diffractograms, indicating agreement with other silver XRD traces that this is the main peak representing the silver seed base units.[2,34]

A few measurements were performed using atomic force microscopy (AFM). These were challenging due to limited local

capabilities, but tAgNP thickness measurements ranged from 6 to 13 nm, with the lower values for triangles in the 50–70 nm range and the large ones for particles over 100 nm.

TEM images were collected using an FEI Tecnai G2 Spirit Twin TEM, and average particle sizes were estimated from the measurements of 150–200 individual particles per sample, or as many as could be visualized in the cases of dispersed or heavily clustered TEM samples such as, respectively, green LED-synthesized tAgNPs and dAgNPs.

Data availability

The data supporting this article have been included as part of the ESI.†

Conflicts of interest

There are no conflicts to declare. However, we would like to disclose that some of the Luzchem equipment used is manufactured by Luzchem Research, Inc. where JCS is a co-founder (1997) but has no financial interests at present.

Acknowledgements

This work was supported by the Natural Sciences and Engineering Research Council of Canada, the Canada Foundation for Innovation and the Canada Research Chairs Program. Thanks are due to Luzchem Research Inc., for providing spectral data for the light sources and for the gift of two well-plate illuminators.

Notes and references

1 M. K. Rai, S. D. Deshmukh, A. P. Ingle and A. K. Gade, Silver nanoparticles: the powerful nanoweapon against multidrug-resistant bacteria, *J. Appl. Microbiol.*, 2012, **112**, 841–852.
2 C. R. Bourgonje, D. Regis Correa da Silva, E. McIlroy, N. D. Calvert, A. J. Shuhendler and J. C. Scaiano, Silver Nanoparticles with exceptional near-infrared absorbance for photo-enhanced antimicrobial applications, *J. Mater. Chem. B*, 2023, **11**, 6114–6122.
3 M. Singhal, L. Loveleen, R. Manchanda, A. Syed, A. H. Bahkali, L. S. Wong, S. Nimesh and N. Gupta, Design, synthesis and optimization of silver nanoparticles using Azadirachta indica bark extract and its antibacterial application, *J. Agric. Food Res.*, 2024, **16**, 101088.
4 A. Menichetti, A. Mavridi-Printezi, D. Mordini and M. Montalti, *J. Funct. Biomater.*, 2023, 244.
5 O. Gherasim, R. A. Puiu, A. C. Bîrcă, A.-C. Burduşel and A. M. Grumezescu, *Nanomaterials*, 2020, 2318.
6 H. D. Beyene, A. A. Werkneh, H. K. Bezabh and T. G. Ambaye, Synthesis paradigm and applications of silver nanoparticles (AgNPs), a review, *Sustainable Mater. Technol.*, 2017, **13**, 18–23.
7 A. A. Yaqoob, K. Umar and M. N. M. Ibrahim, Silver nanoparticles: various methods of synthesis, size affecting factors and their potential applications–a review, *Appl. Nanosci.*, 2020, **10**, 1369–1378.
8 M. Yaghmaei, C. R. Bourgonje and J. C. Scaiano, Facile Scale-Up of the Flow Synthesis of Silver Nanostructures Based on Norrish Type I Photoinitiators, *Molecules*, 2023, **28**, 4445.
9 K. G. Stamplecoskie and J. C. Scaiano, Light Emitting Diode Irradiation Can Control the Morphology and Optical Properties of Silver Nanoparticles, *J. Am. Chem. Soc.*, 2010, **132**, 1825–1827.
10 A. A. Furletov, V. V. Apyari, V. D. Zaytsev, A. O. Sarkisyan and S. G. Dmitrienko, Silver triangular nanoplates: Synthesis and application as an analytical reagent in optical molecular spectroscopy. A review, *Trends Anal. Chem.*, 2023, **166**, 117202.
11 J. Singh and A. S. Dhaliwal, Plasmon-induced photocatalytic degradation of methylene blue dye using biosynthesized silver nanoparticles as photocatalyst, *Environ. Technol.*, 2020, **41**, 1520–1534.
12 P. Rani, V. Kumar, P. P. Singh, A. S. Matharu, W. Zhang, K.-H. Kim, J. Singh and M. Rawat, Highly stable AgNPs prepared *via* a novel green approach for catalytic and photocatalytic removal of biological and non-biological pollutants, *Environ. Int.*, 2020, **143**, 105924.
13 B. Zhou and D. Yan, Precise metal nanoclusters: Linking the atomic world to photonic applications, *Matter*, 2023, **6**, 3126–3129.
14 L. G. Rodriguez Barroso, E. Lanzagorta Garcia, M. Mojicevic, M. Huerta, R. Pogue, D. M. Devine and M. Brennan-Fournet, Triangular Silver Nanoparticles Synthesis: Investigating Potential Application in Materials and Biosensing, *Appl. Sci.*, 2023, **13**, 8100.
15 S. Kaur, R. Dadwal, H. Nandanwar and S. Soni, Limits of antibacterial activity of triangular silver nanoplates and photothermal enhancement thereof for Bacillus subtilis, *J. Photochem. Photobiol., B*, 2023, **247**, 112787.
16 J. J. Mock, M. Barbic, D. R. Smith, D. A. Schultz and S. Schultz, Shape effects in plasmon resonance of individual colloidal silver nanoparticles, *J. Chem. Phys.*, 2002, **116**, 6755–6759.
17 S. Eustis and M. A. El-Sayed, Why gold nanoparticles are more precious than pretty gold: Noble metal surface plasmon resonance and its enhancement of the radiative and nonradiative properties of nanocrystals of different shapes, *Chem. Soc. Rev.*, 2006, **35**, 209–217.
18 D. R. Mota, G. A. S. Lima, G. B. Helene and D. S. Pellosi, Tailoring Nanoparticle Morphology to Match Application: Growth under Low-Intensity Polychromatic Light Irradiation Governs the Morphology and Optical Properties of Silver Nanoparticles, *ACS Appl. Nano Mater.*, 2020, **3**, 4893–4903.
19 A. Bouafia, S. E. Laouini, A. S. A. Ahmed, A. V. Soldatov, H. Algarni, K. Feng Chong and G. A. M. Ali, *Nanomaterials*, 2021, 2318.
20 X. Zhu, X. Zhuo, Q. Li, Z. Yang and J. Wang, Gold Nanobipyramid-Supported Silver Nanostructures with Narrow Plasmon Linewidths and Improved Chemical Stability, *Adv. Funct. Mater.*, 2016, **26**, 341–352.

21 H. Li and H. Xu, Mechanisms of bacterial resistance to environmental silver and antimicrobial strategies for silver: A review, *Environ. Res.*, 2024, **248**, 118313.
22 N. Serginay, A. N. Dizaji, H. Mazlumoglu, E. Karatas, A. Yilmaz and M. Yilmaz, Antibacterial activity and cytotoxicity of bioinspired poly(L-DOPA)-mediated silver nanostructure-decorated titanium dioxide nanowires, *Colloids Surf., A*, 2022, **639**, 128350.
23 B.-M. Chang, L. Pan, H.-H. Lin and H.-C. Chang, Nanodiamond-supported silver nanoparticles as potent and safe antibacterial agents, *Sci. Rep.*, 2019, **9**, 13164.
24 G. Gunaydin, M. E. Gedik and S. Ayan, Photodynamic Therapy—Current Limitations and Novel Approaches, *Front. Chem.*, 2021, **9**, 1–25.
25 T. H. N. Nguyen, T. D. Nguyen, M. T. Cao and V. V. Pham, Fast and simple synthesis of triangular silver nanoparticles under the assistance of light, *Colloids Surf., A*, 2020, **594**, 124659.
26 M. Yaghmaei and J. C. Scaiano, A simple Norrish Type II actinometer for flow photoreactions, *Photochem. Photobiol. Sci.*, 2023, **22**, 1865–1874.
27 A. Albini, Some remarks on the first law of photochemistry, *Photochem. Photobiol. Sci.*, 2016, **15**, 319–324.
28 L. Zhang, Y. Zhao, Z. Lin, F. Gu, S. P. Lau, L. Li and Y. Chai, Kinetically controlled synthesis of large-scale morphology-tailored silver nanostructures at low temperature, *Nanoscale*, 2015, **7**, 13420–13426.
29 V. V. Pinto, M. J. Ferreira, R. Silva, H. A. Santos, F. Silva and C. M. Pereira, Long time effect on the stability of silver nanoparticles in aqueous medium: Effect of the synthesis and storage conditions, *Colloids Surf., A*, 2010, **364**, 19–25.
30 J. C. Scaiano, K. G. Stamplecoskie and G. L. Hallett-Tapley, Photochemical Norrish type I reaction as a tool for metal nanoparticle synthesis: importance of proton coupled electron transfer, *Chem. Commun.*, 2012, **48**, 4798–4808.
31 K. L. McGilvray, M. R. Decan, D. Wang and J. C. Scaiano, Facile Photochemical Synthesis of Unprotected Aqueous Gold Nanoparticles, *J. Am. Chem. Soc.*, 2006, **128**, 15980–15981.
32 J. Belloni, The role of silver clusters in photography, *C. R. Phys.*, 2002, **3**, 381–390.
33 A. Sánchez-Iglesias, N. Winckelmans, T. Altantzis, S. Bals, M. Grzelczak and L. M. Liz-Marzán, High-Yield Seeded Growth of Monodisperse Pentatwinned Gold Nanoparticles through Thermally Induced Seed Twinning, *J. Am. Chem. Soc.*, 2017, **139**, 107–110.
34 B. Lafuente, R. T. Downs, H. Yang and N. Stone, *The Power of Databases: the RRUFF Project*, W. De Gruyter, Berlin, 2015.